the structure of the material without giving rise to the formation of domains. If we use the variable, ρh, which describes the density fluctuations of a given wave vector, then we can view the position of the local fluctuations as a set of collective coordinates. It is under such circumstances that the RPA was introduced and is a mathematical tool similar to a variety of others developed for the expressed purpose of reducing intractable mathematical equations such that simple approximate solutions can be obtained. On the other hand, its use imposes certain constraints upon the system's response and in particular assumes only weak interaction.

The physics behind the RPA may be best illustrated by the following simple examples.

Since we assume that $\chi_{ij}^0(\mathbf{r})$ is proportional to the pair correlation function $P_{ij}^0(\mathbf{r})$ for two monomers in the absence of an external potential, then it can be expected that the presence of one perturbation at the k'th position will influence the i'th position (where k and i may be either on the same chain or on different chains). If one now considers these perturbations as a set of plane waves, χ_j, interacting with a set of lattice sites, then the major effect in terms of scattering should occur when a critical condition exists between the plane waves and the lattice. This is then similar to the Debye–Sears photon–phonon problem. However, due to the fact that some of the lattice sites are interconnected by molecular chemical bonds and others by van de Waals forces, the overall response will be biased. In particular, cross-linked materials, where the cross-linking sites are the scatterers, will represent one extreme where due to chemical connectivity any adjustments must be accommodated by changes in the chain's configuration. Very short diterminated chains represent the other extreme because such effects will be couched in intramolecular considerations due to geometric packing. We refer those who are more interested in the RPA to ref 8 and 9.

Acknowledgment. We would like to thank Professor deGennes for suggesting this approach and for discussions about his work and Dr. J. Bendler for a critical reading of this work.

References and Notes

(1) G. G. Vitale and D. G. LeGrande, *Macromolecules*, **9**, 749 (1976).
(2) A. D. LeGrand, G. G. Vitale, and D. G. LeGrand, *Polym. Eng. Sci.*, **17**, (1977).
(3) P. G. deGennes, *J. Phys. (Paris)*, **31**, 235 (1970).
(4) G. Jannink and P. G. deGennes, *J. Chem. Phys.* **48**, 2260 (1968).
(5) G. Brady, E. Wallerman, and J. Wellendorf, *J. Chem.*, **47**, 855 (1967).
(6) G. Brady, C. Cohen-Addad, and E. F. Lyden, *J. Chem. Phys.*, **51**, 4309 (1969).
(7) F. Boue, M. Daoud, M. Nierlich, G. Williams, J. P. Cotton, B. Farnous, H. Benoit, R. Duplessix, and C. Picot, *Inter. Atomic Energy Agency* 1, 563–588 (1978).
(8) D. Pines and P. Nozières, "Theory of Quantum Fluids", W. A. Benjamin, New York, 1966.
(9) N. A. March and M. P. Tosi, "Atomic Dynamics in Liquids", Halstead Press, New York, 1976.
(10) A copy of this program is available upon request.

Molecular Thermodynamics of Polymer Compatibility: Effect of Contact Agility

D. D. Liu and J. M. Prausnitz*

Department of Chemical Engineering, University of California—Berkeley, Berkeley, California 94720. *Received November 30, 1978*

ABSTRACT: While the influence of interaction energy on polymer–polymer compatibility has long been recognized, little explicit attention has been given to the influence of "structural effects", i.e., of component contact agility, c/q. Calculated phase equilibria are shown for some polymer–polymer and some polymer–polymer–solvent systems using a perturbed-hard-chain theory. This theory predicts an LCST-type phase diagram for a polymer–polymer binary mixture when the contact agilities for polymers are different even though all energy parameters are identical. For ternary systems containing two polymers and a common solvent, solvent contact agility affects the compatibility differently in the UCST and the LCST region. When solvent contact agility is within a good solvent limit, so that the polymer–solvent binary is completely miscible, the lower contact-agility solvent is more efficient in the LCST region; however, the opposite holds in the UCST region.

It has long been recognized that the configurational entropy of mixing for a polymer–polymer mixture is much smaller than that for a mixture of ordinary liquids. A small, positive enthalpy of mixing is sufficient for phase separation; therefore, mutually soluble polymer pairs are the exception, rather than the rule. Several authors have discussed the thermodynamics of polymer–polymer mixtures,[1–4] using classical Flory–Huggins theory wherein the parameter χ_{12} plays a central role.

As shown by Flory and others,[3,5–9] the main defect of the classical theory follows from its failure to take into account the free-volume effect or, in Flory's words, "equation-of-state contributions to the free energy of mixing". These free-volume effects are responsible for partial miscibility at *high* temperatures, leading to a *lower* critical solution temperature (LCST).

As shown by Flory and others,[3,10] free-volume effects in mixtures can be quantitatively described through an equation of state of the van der Waals type, coupled with Prigogine's assumption that at liquid-like densities external rotational and vibrational degrees of freedom can be considered as equivalent translational degrees of freedom.[10]

McMaster[11] and Patterson and Robard[12] have applied the Flory–Prigogine theory to the thermodynamics of polymer compatibility. According to Patterson, for a mixture containing polymer 1 and polymer 2, the Flory–Huggins parameter χ_{12} can be approximated by the sum of two terms

0024-9297/79/2212-0454$01.00/0

$$\chi_{12} = \underbrace{\frac{(-U_1)}{RT}\frac{X_{12}}{P_1^*}}_{\text{contact-energy contribution}} + \underbrace{\frac{C_{p,1}}{2R}\left(1 - \frac{T_1^*}{T_2^*}\right)^2}_{\text{free-volume contribution}} \qquad (1)$$

where $(-U_1)$ is the positive molar configurational energy of component 1, taken as reference fluid, $C_{p,1}$ stands for the configurational heat capacity, P_1^* represents the characteristic pressure of component 1, and T^* stands for the characteristic temperature:

$$T^* = (\epsilon/k)/(c/q) \qquad (2)$$

where ϵ/k is the interaction potential energy (expressed in absolute temperature units), c is one-third of the number of external degrees of freedom per molecule, and q is proportional to a molecule's surface area. As defined by Flory, binary parameter X_{12} accounts for the interaction energy change

$$X_{12} = \frac{q_1}{2r_1{v^*_{\text{seg}}}^2}(\epsilon_{11} + \epsilon_{22} - 2\epsilon_{12}) \qquad (3)$$

where r is the number of segments per molecule, v^*_{seg} is the hard-core volume of a unit segment, and ϵ_{ij} represents the interaction potential energy between a segment from molecule i and a segment from molecule j.

In eq 1, the first term may be positive or negative (depending on the sign of X_{12}) but the second term is always positive or zero. Phase separation occurs when

$$\chi_{12} = \tfrac{1}{2}[1 + (r_1/r_2)^{1/2}]^2 \qquad (4)$$

Equations 1 and 4 indicate that two polymers may be compatible if X_{12} is small or negative (a negative X_{12} stands for strong attraction between components 1 and 2) and if, in addition, $T_1^* \approx T_2^*$.

To meet the second condition, eq 2 shows that it is not necessary that $\epsilon_1 \approx \epsilon_2$ since the definition of T^* also includes c/q. The influence of c/q on solution properties has earlier been called "structural effects".[10] For a more heuristic description, we refer to the ratio c/q as the contact agility.

We are here concerned with the effect of contact agility on polymer compatibility in binary systems; we also discuss polymer compatibility in a ternary system containing two incompatible polymers and one common solvent. Our analysis is based on the perturbed-hard-chain theory[13-17] which, while different in detail, is similar to the Flory–Prigogine theory.

Perturbed-Hard-Chain Theory

As discussed by Beret and Prausnitz,[13] the canonical partition function for a pure fluid, applicable over the entire range of gas and liquid densities, is given by

$$Q(N,V,T) = \frac{1}{N!}\left(\frac{V_f}{\Lambda^3}\right)^N (\omega_{r,v})_{\text{int}}{}^N(\omega_{r,v})_{\text{ext}}{}^N \exp\left(-\frac{N\phi}{2kT}\right) \qquad (5)$$

where N is the number of molecules at temperature T and volume V; Λ is the thermal de Broglie wavelength; V_f is the free volume; ϕ is the potential field; k stands for the Boltzmann constant; and $\omega_{r,v}$ represents contributions from rotational and vibrational degrees of freedom. Following Prigogine, the rotational and vibrational contribution is factored into internal and external parts; the internal part depends only on temperature.

At liquid-like densities, the external vibrational and rotational degrees of freedom are considered to be equivalent translational degrees of freedom. The total number of external degrees of freedom is $3c$ per molecule. For argon-like molecules, c is unity; for molecules of more complex shape, c is larger than unity.

For the entire fluid range, Beret and Prausnitz proposed the approximation

$$(\omega_{r,v})_{\text{ext}} = (V_f/V)^{c-1} \qquad (6)$$

Equation 6 assures that the equation of state derived from eq 5 approaches the correct ideal-gas limit as the density goes to zero and approaches a Flory–Prigogine type of equation of state when the density goes to that of a close-packed liquid.

For the free volume, Beret and Prausnitz used the hard-sphere fluid equation of Carnahan and Starling; for the potential field ϕ, they used the molecular-dynamics results of Alder et al.[19] The resulting partition function contains three independent parameters: the characteristic pressure P^*, the specific molecular core volume v^*_{sp}, and the characteristic temperature T^*, defined by eq 2.

The characteristic pressure is defined by

$$P^* = \frac{\epsilon}{k}\frac{qR}{rv^*_{\text{seg}}} \qquad (7)$$

where R is the gas constant. The two hard-core volumes (v^*_{sp} and v^*_{seg}) are related to r, the number of segments, by

$$r = v^*_{\text{sp}}M/v^*_{\text{seg}} \qquad (8)$$

where M is the molecular weight. For pure fluids, we determine P^*, v^*_{sp}, and T^* from vapor-pressure and/or P–V–T data.

While pure-component data give us T^*, some additional assumptions are required to find ϵ/k and c/q separately. Following Donohue,[14] for all components we arbitrarily set v^*_{seg} to be 9.6 cm^3/mol which corresponds to the hard-core volume of a $-CH_2-$ unit in a long-chain paraffin. Donohue sets ϵ/k for normal alkanes to be 105 K; this follows from setting $q = 0.724$ for a $-CH_2-$ segment. For other fluids, optimal values for ϵ/k are determined from an over-all study of experimental binary data; r is obtained from v^*_{sp}, v^*_{seg}, and M using eq 8. Parameters c and q are then obtained from ϵ/k, r, and P^* using eq 2 and 8.

When extended to mixtures, the partition function given by eq 5 must meet the following boundary conditions:

(1) The second virial coefficient must be a quadratic function of the mole fractions.

(2) At high densities, the athermal entropy of mixing must reduce to the Flory–Huggins entropy of mixing when the ratio of volume to hard-core volume is independent of composition.

(3) We define an excess quantity as one relative to the ideal gas at the same volume, temperature, and composition. The excess chemical potential of a monomer in a highly concentrated polymer solution must remain finite as the polymer chain becomes infinitely long.

(4) To take into account molecular clustering when the mixture contains molecules (or segments) with significantly different potential energies, the Helmholtz energy derived from the partition function must be consistent with the perturbation-theory results of Henderson[20] for mixtures of spherical molecules.

To meet these conditions, the Helmholtz energy A is expanded in reciprocal temperature:

$$A - A(\text{ideal gas}) = A^{(0)} + \frac{A^{(1)}}{T} + \frac{A^{(2)}}{T^2} + \frac{A^{(3)}}{T^3} + \frac{A^{(4)}}{T^4} \qquad (9)$$

The leading term $A^{(0)}$ is the hard-chain, repulsive-force term. It is found from a one-fluid extension to mixtures of the hard-sphere equation of Carnahan and Starling[18]

$$\frac{A^{(0)}}{NkT} = -\frac{N\langle c\rangle(3\tau\tilde{\rho} - 4)\tau\tilde{\rho}}{(1 - \tau\tilde{\rho})^2} \tag{10}$$

where $\tau = 0.7405$ and $\tilde{\rho}$ is the reduced density

$$\tilde{\rho} = \langle v^*\rangle/v \tag{11}$$

The bracketed quantities in eq 10 and 11 are mole-fraction averaged quantities for the mixture.

Higher-order terms in eq 9 represent contributions from attractive forces. They have the form:

$$A^{(l)} = f^{(l)}(\tilde{\rho},\langle T^{*l}\rangle,\langle c\rangle) \tag{12}$$

$$l = 1, 2, 3, 4$$

The functions $f^{(l)}$ are extensions of those given by Alder et al.[19] The composition averages for $\langle T^{*l}\rangle$ depend on l; details are given in the supplementary material.

The chemical potential of component j can be calculated from the thermodynamic relation

$$\mu_j = \left(\frac{\partial A}{\partial N_j}\right)_{N_i(i\neq j),T,V} \tag{13}$$

Phase-equilibrium calculations in mixtures require pure-component parameters (P^*, v^*_{sp}, T^*, r, ϵ/k) and one binary constant k_{ij} defined by

$$\epsilon_{ij} = (\epsilon_i\epsilon_j)^{1/2}(1 - k_{ij}) \tag{14}$$

Interaction potential energies ϵ_{ij}, ϵ_i, and ϵ_j are needed to calculate $\langle T^{*l}\rangle$. In our discussion, binary parameter k_{ij} is assumed to be independent of temperature, density, and composition. Equations for the chemical potential are shown in the supplementary material.

Phase-Equilibrium Calculations

Some representative phase equilibria have been calculated for realistic model molecules at 1 atm and at temperatures from 0 to 300 °C. Pure-component parameters are obtained from experimental data for typical polymers. We are particularly concerned with the separate effect of differences in ϵ/k's and c/q's on polymer–polymer and polymer–polymer–solvent phase behavior. In our calculations we use for polymer parameters those for PMMA [poly(methyl methacrylate)]: $P^* = 1293$ bars, $v^*_{\mathrm{sp}} = 0.4775$ cm^3/g, and $T^* = 554$ K. Molecular weights of all polymers are 10^4 g/mol. The molecular weight of the solvent is set at 500 or 1000 g/mol; these relatively high values are used because, for practical application, the solvent must have low volatility.

Results

Figure 1 shows the phase diagram for three binary mixtures. Each of these contains two monodisperse polymers, A and B. For both A and B, parameter ϵ/k is arbitrarily set at 112.5 K; binary parameter $k_{\mathrm{AB}} = 0$. However, c/q for polymer A is not the same as that for polymer B. Figure 1 shows that phase separation occurs at high temperatures due to the difference in contact agility.

At fixed temperature, mutual solubility rises as the difference in c/q falls. The calculations show only a lower critical solution temperature; there is no upper critical solution temperature.

Within the framework of the Flory–Patterson theory, the results shown in Figure 1 could also have been obtained by keeping c/q constant and changing ϵ. However, this conclusion does not hold for our (PHCT) treatment because, in contrast to Flory–Patterson theory, PHCT contains higher terms (in T^{-1}) in the perturbation expansion (eq 9).

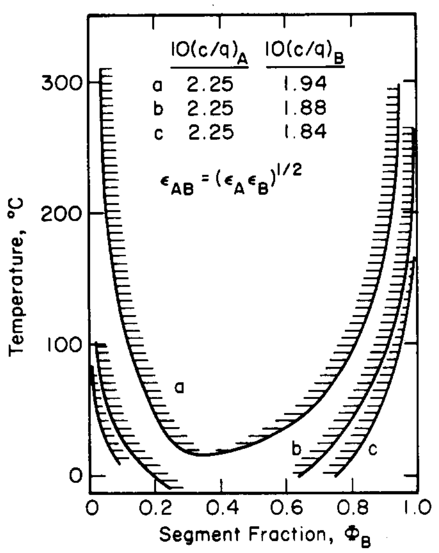

Polymer	P^* bars	v^*_{SP} cm^3/g	T^*,K	ϵ/k, K	10 c/q
A	1293	0.4775	500	112.5	2.25
B, line a	1293	0.4775	580	112.5	1.94
B, line b	1293	0.4775	600	112.5	1.88
B, line c	1293	0.4775	610	112.5	1.84

Figure 1. Immiscibility of a polymer A–polymer B mixture at high temperatures due to contact agility differences.

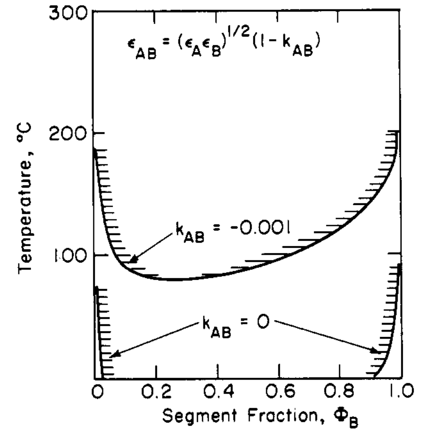

Polymer	P^* bars	v^*_{SP} cm^3/g	T^*,K	ϵ/k, K	10 c/q	MW
A	1293	0.4775	500	112.5	2.25	10^4
B	1293	0.4775	650	112.5	1.73	10^4

Figure 2. Change of phase diagram resulting from a small increase in ϵ_{AB} when $\epsilon_{\mathrm{A}} = \epsilon_{\mathrm{B}}$.

As shown earlier by Patterson,[12] a small change in ϵ_{AB} may have a drastic effect on the phase diagram. We confirm this effect, as is shown in Figures 2, 3, and 4. Figure 2 indicates that an increase of 0.1% in ϵ_{AB} raises the lower critical solution temperature by more than 100 °C. Figure 3 shows that two polymers which are compatible below 100 °C when $k_{\mathrm{AB}} = 0$ become incompatible when $k_{\mathrm{AB}} = +0.001$. In Figure 4, both lower and upper critical solution temperatures appear when ϵ_{A} and ϵ_{B} are different and $k_{\mathrm{AB}} = -0.004$. The two polymers which are compatible between 75 and 160 °C become incompatible when k_{AB} changes from -0.004 to -0.003.

For a ternary system, Figures 5 and 6 show the effect of solvent, c/q. In the LCST region, mutual solubility of

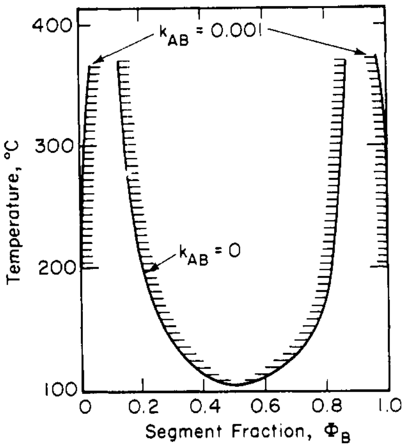

Polymer	P^* bars	v^*_{SP} cc/g	T^*,K	ϵ/k,K	10 c/q	MW
A	1293	0.4775	500	112.5	2.25	10^4
B	1293	0.4775	570	112.5	1.97	10^4

Figure 3. Change of phase diagram resulting from a small change in ϵ_{AB} when $\epsilon_A = \epsilon_B$.

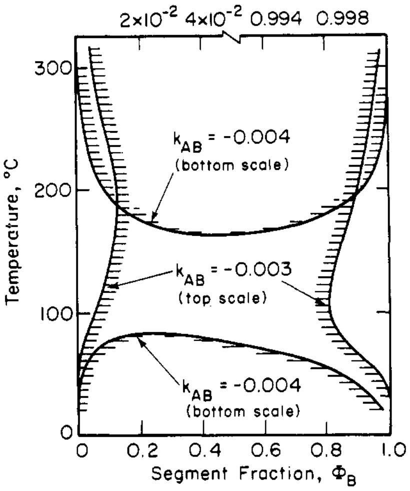

Polymer	P^* bars	v^*_{SP} cm^3/g	T^*,K	ϵ/k,K	10 c/q	MW
A	1293	0.4775	500	112.5	2.25	10^4
B	1494	0.4775	659	130.0	1.97	10^4

Figure 4. Change of phase diagram resulting from a small change in ϵ_{AB} when $\epsilon_A \neq \epsilon_B$.

the two polymers is more efficiently enhanced by solvents with lower c/q values. However, in the UCST region, the effect of the solvent c/q is different; in Figure 6, the minimum solvent segment fractions required for compatibility first decrease and then increase as solvent c/q rises. Figure 6 also shows the effect of solvent–polymer interaction potential. Polymer compatibility does not change significantly when the polymer–solvent interaction potential increases by 2%.

Figures 7 and 8 show the effect of solvent interaction potential energies in the LCST and UCST regions, respectively. The calculated curves with $k_{ps} = 0$ in Figures 7 and 8 show a distinct minimum when the solvent interaction potential is close to the arithmetic mean of those for the two polymers. The amount of solvent required for compatibility may be significantly decreased by raising the polymer–solvent attraction potential, ϵ_{ps}, when the solvent ϵ is not close to the arithmetic mean of those of the two polymers. When solvent ϵ is close to the arithmetic mean, an increase in ϵ_{ps} produces little change in the amount of solvent required for compatibility.

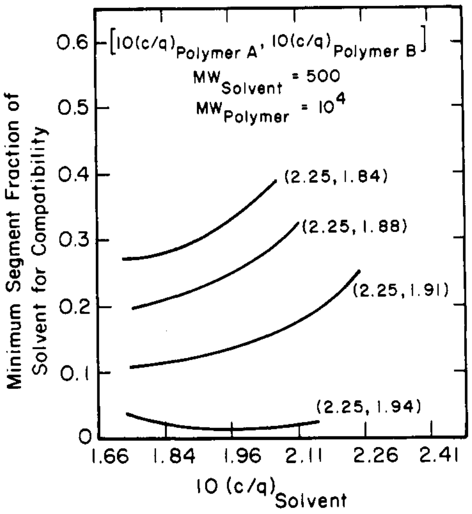

	P^* bars	v^*_{SP} cm^3/g	T^*,K	ϵ/k,K	10 c/q
Polymer A	1293	0.4775	500	112.5	2.25
Polymer B	1293	0.4775	-	112.5	-
Solvent S	1293	0.4775	-	112.5	-

$k_{AB} = k_{AS} = k_{BS} = 0$

Figure 5. Effect of component contact agility on solvent content required for compatibility in the LCST region at 50 °C (1 atm).

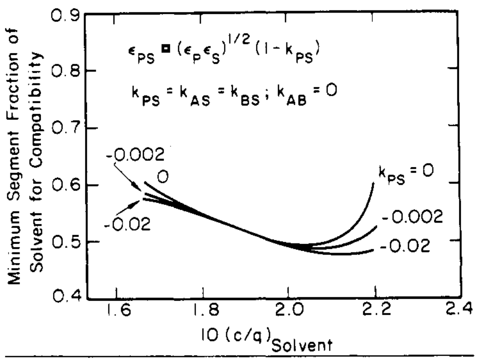

	P^* bars	v^*_{SP} cm^3/g	T^*,K	ϵ/k,K	10 c/q	MW
Polymer A	1293	0.4775	500	100	2.09	10^4
Polymer B	1422	0.4775	550	110	2.09	10^4
Solvent S	1357	0.4775	-	105	-	10^3

$k_{PS} = k_{AS} = k_{BS}$; $k_{AB} = 0$.

Figure 6. Effect of solvent agility and solvent–polymer potential energy on solvent content required for compatibility in the UCST region at 100 °C.

Discussion

As shown by McMaster[11] and by Patterson and Robard,[12] a small change in the polymer–polymer interaction potential can change the binary phase diagram drastically. However, when the contact agilities are different, the perturbed-hard-chain theory predicts LCST-type phase diagrams even for those polymer–polymer mixtures where the contact energies are the same. In other words, the condition $\epsilon_A = \epsilon_B = \epsilon_{AB}$ is not necessarily sufficient to achieve compatibility, as has been pointed out previously.[11,12] This is consistent with the Patterson–Robard analysis of the Prigogine–Flory theory. When contact energies are the same, eq 1 becomes

$$\chi_{12} = \frac{C_{p,1}}{2R}\left(1 - \frac{(c/q)_2}{(c/q)_1}\right)^2 \tag{15}$$

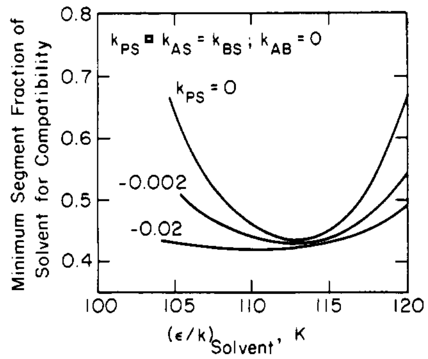

	P^* bars	v^*_{sp} cm^3/g	T^*, K	ϵ/k, K	10 c/q	MW
Polymer A	1293	0.4775	500	112.5	2.25	10^4
Polymer B	1293	0.4775	600	112.5	1.875	10^4
Solvent S	–	0.4775	–	–	2.045	10^3

$k_{PS} = k_{AS} = k_{BS}$; $k_{AB} = 0$.

Figure 7. Effect of potential energies on the solvent content required for compatibility in the LCST region at 100 °C.

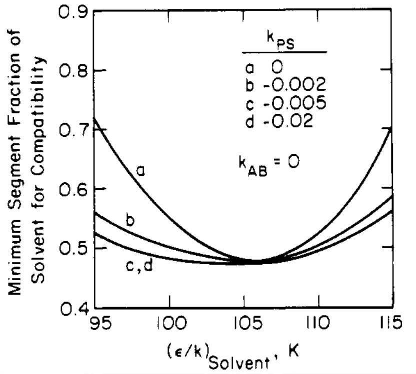

	P^* bars	v^*_{sp} cm^3/g	T^*, K	ϵ/k, K	10 c/q	MW
Polymer A	1293	0.4775	500	100	2.00	10^4
Polymer B	1422	0.4775	550	110	2.00	10^4
Solvent S	–	0.4775	–	–	2.00	10^3

Figure 8. Effect of potential energies on the solvent content required for compatibility in the UCST region at 100 °C.

Since $C_{p,1}$ is an increasing function of temperature, χ_{12} will exceed its initial value defined by eq 4 at high temperature when contact agilities of two polymers are not identical.

It is well known that the mutual solubility of two polymers can be increased by adding a common solvent to the mixture; two polymers may become compatible if a sufficient amount of solvent is added. The efficiency of this solvent effect depends not only on the solvent molecular size and the solvent interaction potential energy but also on the solvent contact agility.

A low-molecular-weight solvent is more efficient due to favorable configurational entropy of mixing. In our calculations, we add a comparatively heavy solvent ($M = 500$ or 1000) to the polymer mixture because we want the vapor pressure of the solvent to be low.

The solvent contact agility effect for LCST-type polymer pairs is different from that for UCST-type polymer pairs. Solvent agility must be within a "good solvent" limit so that the polymer–solvent binary mixture is completely miscible. When c/q is within this limit, the lower-contact-agility solvent is more efficient in the LCST region; however, the opposite holds in the UCST region. This conclusion is qualitatively consistent with Flory–Patterson theory if we recall that a decrease of solvent contact agility decreases the reduced temperature; this decrease enhances polymer–polymer mutual solubility in the LCST region but makes polymers less miscible in the UCST region.

In a polymer–polymer–solvent system, the effect of the polymer–solvent interaction energy is not as strong as that of the polymer–polymer interaction energy. Changing a good solvent to a "better" one by increasing the solvent–polymer interaction potential energy does not drastically change polymer–polymer mutual solubility.

The calculations shown here are made for monodisperse polymers. The effect of polydispersity has been considered by several authors, notably by Koningsveld[21,22] who calls attention to the possible strong influence of the effect of concentration on the radius of gyration.

The works discussed here suggest that if a low-molecular-weight hump exists in the molecular-weight distribution, compatibility is enhanced because of favorable combinatorial entropy. That conclusion is surely not surprising. However, our theoretical treatment also shows that a low-molecular-weight hump of the polymer having the lower c/q enhances miscibility more if the two polymers are above the LCST; on the other hand, the low-molecular-weight hump of the polymer with the higher c/q enhances miscibility more if the two polymers are below the UCST.

Acknowledgment. The authors are grateful to T. F. Anderson for helpful discussions and to the National Science Foundation and the donors of the Petroleum Research Fund, administered by the American Chemical Society, for financial support.

Supplementary Material Available: Tabulations for universal constants for attractive force contributions and in the second virial coefficient correction term and equations for chemical potential (8 pages). Ordering information is given on any current masthead page.

References and Notes

(1) R. L. Scott, *J. Chem. Phys.*, **17**, 279 (1949).
(2) H. Tompa, *Trans. Faraday Soc.*, **45**, 1140 (1949).
(3) L. Zeman and D. Patterson, *Macromolecules*, **5**, 513 (1972).
(4) C. C. Hsu and J. M. Prausnitz, *Macromolecules*, **7**, 320 (1974).
(5) P. J. Flory, *J. Am. Chem. Soc.*, **87**, 1833 (1965).
(6) D. Patterson and G. Delmas, *Trans. Faraday Soc.*, **65**, 708 (1969).
(7) D. Patterson, G. Delmas, and T. Somcynsky, *Polymer*, **8**, 503 (1967).
(8) K. S. Siow, G. Delmas, and D. Patterson, *J. Phys. Chem.*, **76**, 1206 (1972).
(9) L. Zeman, J. Biros, G. Delmas, and D. Patterson, *J. Phys. Chem.*, **76**, 1206 (1972).
(10) I. Prigogine, "Molecular Theory of Solutions", North-Holland Press, Amsterdam, 1957, Chapter XVI.
(11) L. P. McMaster, *Macromolecules*, **5**, 760 (1973).
(12) D. Patterson and A. Robard, *Macromolecules*, **10**, 690 (1978).
(13) S. Beret and J. M. Prausnitz, *AIChE J.*, **21**, 1123 (1975).
(14) M. D. Donohue and J. M. Prausnitz, *AIChE J.*, **24**, 849 (1978).
(15) J. Gmehling, D. D. Liu, and J. M. Prausnitz, *J. Chem. Eng. Sci.*, in press.
(16) D. D. Liu and J. M. Prausnitz, *J. Appl. Polym. Sci.*, in press.
(17) D. D. Liu and J. M. Prausnitz, *Ind. Eng. Chem., Prod. Res. Dev.*, in press.
(18) N. F. Carnahan and K. E. Starling, *J. Chem. Phys.*, **51**, 639 (1969).
(19) B. J. Alder, D. A. Young, and M. A. Mark, *J. Chem. Phys.*, **56**, 3013 (1972).
(20) D. Henderson, *J. Chem. Phys.*, **61**, 926 (1974).
(21) R. Koningsveld and L. A. Kleintjens, *Br. Polym. J.*, **9**, 212 (1977).
(22) R. Koningsveld, Yugoslav Symposium on Macromolecules, Novi Sad, January 1979.